MECHANICAL PROPERTIES OF GRAPHENE OXIDE REINFORCED ALUMINIUM MATRIX COMPOSITES

Bhagya Lakshmi Dasari[1], Muhammad Morshed[2], Jamshid M Nouri[1], Dermot Brabazon[3] and Sumsun Naher[1] *

[1]Department of Mechanical Engineering and Aeronautics, City, University of London, London, UK

[2]Dynex Semiconductor Ltd, Doddington Road, Lincoln, UK

[3] Advanced Processing Technology Research Centre, School of Mechanical and Manufacturing Engineering, Dublin City University, Dublin, Ireland

ABSTRACT

In this paper, the properties of powder metallurgy produced samples of GO reinforced aluminium composites were examined. Discs of 20 mm diameter and 0.5 mm thickness were made from pure Al powder of 35 µm particle size and with GO reinforcement at different GO wt% (0.05, 0.1 and 0.2). The mixture of Al/GO powders prepared through liquid infiltration were cold compacted and then sintered. The GO reinforced Al matrix composites were characterised using the scanning electron microscope with energy dispersion spectroscopy (SEM/EDX) for investigation of the homogeneous dispersion of GO into the matrix. X-ray diffraction (XRD) analysis for crystallographic phase and micro-Raman spectroscopy was used to identify the phases inside the composite matrix after the sintering process. Micro hardness and the strength values from the produced Al/GO composites were recorded. It is evident from the results obtained that where uniform mixing is achieved, GO reinforced Al composites can be produced with similar hardness values as for those produced from rGO reinforced Al composites.

Keywords: *Metal matrix composites (MMCs), graphene oxide reinforcement, electron microscopy, micro Raman.*

1. INTRODUCTION

The potential improvement in properties achievable from metal matrix composites make them desirable materials in automotive and aerospace industries [1][2]. These include the potential for increased strength, higher elastic modulus, higher service temperature, improved wear resistance, decreased part weight, high electrical and thermal conductivity, low coefficient of thermal expansion and high resistance to thermal fatigue and creep. MMCs were first applied in the production of space craft components, in which high mechanical properties are required for operation in the extreme working environments [3]. The low density of aluminium enables its usage within many MMCs applications, additionally, it is inexpensive in comparison to widely used low density metals such as Ti and Mg [4][5]. High corrosion resistance and better formability makes Al a material used for automobile applications over other alternatives, including ferrous metals. Powder metallurgy or casting are the techniques

*ORCID ID: 0000-0003-2047-5807
E-mail: Sumsun.naher.1@city.ac.uk

generally used to fabricate Al composites with the addition of reinforcement to enhance its properties [6][7][8]. Nano reinforcements such as CNT's and graphene as reinforcement for MMCs have attracted many researchers recently due to their exceptional mechanical [9], thermal [10][11], electrical [12] and tribological [13] properties.

CNT's are promising materials in the design of nano sensors that can be used for precise mechanical and physical properties at micro level that can be extended to nano level which is far from justified. Raffaele et al. [14] have modelled bending armchair CNT's based on gradient elasticity theory, the effect of size on young's modulus was investigated. Emerging applications such as nano-electromechanical systems (NEMS) needs design and optimization of beam like components [15]. Raffaele et al. [16] have identified the need for the design optimization while working with nano materials and have adopted the size effect of nanostructures in nano formulations. The practical engineering applications of CNT's are limited due to the availability of exact solutions for specific cross-sections, it is always challenging to find out the exact solutions for the visco-elastic non-local nano beams made of composite materials under torsion [17]. It can also be noted that the lack of availability of stress- driven systems in order to predict CNT's behaviour under loading limits CNT's applications as the small scale effects in the beams will be neglected [18][19]. CNT's have displayed strengths 10 to 100 times higher than steel, such unique properties in combination with better thermal and electrical properties can lead to the production of promising micro and nano- electro mechanical systems [20] and medicine sector [21].

The recent research carried out on the aluminium matrix composites reinforced with carbon nano tubes [22][23][24] and graphene [25][26][27][28][29] have shown promising increase in mechanical properties which is evident that nano reinforcement for aluminium possess is high potential in future applications. Even though, CNT's enhances the properties of Al matrix composites significantly, the major aspects of uniform dispersion, wetting between the CNT and the base metal still needs more insight. Graphene, a structural element of CNTs is a promising reinforcement for metal matrix composites with a different form factor. Graphene as a reinforcement provides less weight and more strength and high conductivity to the composite material, which possess the potential to replace the conventional materials used in flywheels, cables and even possess a capability to evolve as a strong functional material in energy storage, structural and bio medical fields [30][12]. Its remarkable properties such as Young's modulus of 1 Tpa, fracture strength of 125 Gpa, thermal conductivity of 5000 W/m-k [30] could be used in various applications especially electrical, automobile and aerospace. Graphene oxide (GO) and reduced graphene oxide (rGO), shown in Figure 1 (a) & (b) are the frequently used derivatives of graphene as a reinforcement. Dispersions of GO are very stable in aqueous environments. The use of rGO in the powder state is prone to form agglomeration and is more

*ORCID ID: 0000-0003-2047-5807
E-mail: Sumsun.naher.1@city.ac.uk

hydrophobic in nature. Even though graphene possesses excellent properties, a major drawback to the use of graphene in many applications is its cost.

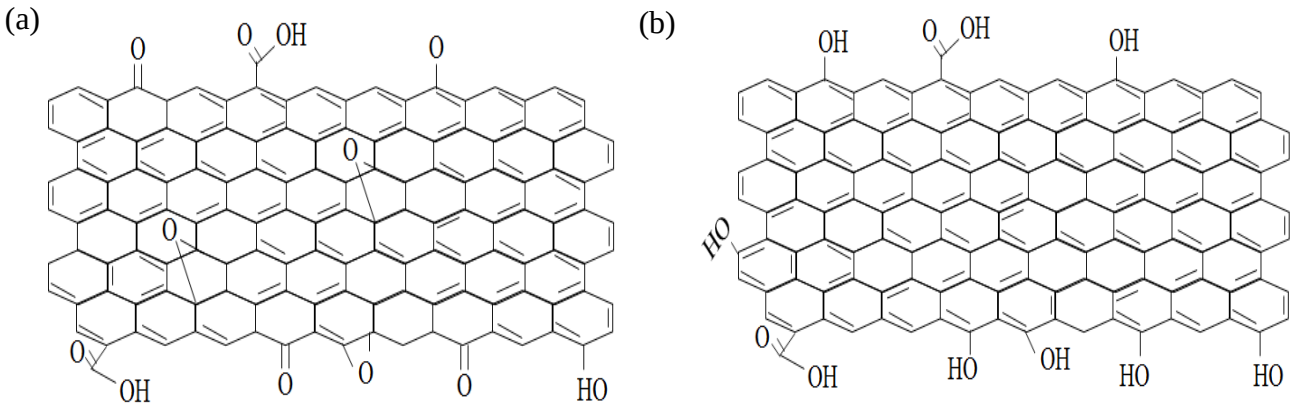

Figure 1: Chemical formulae of graphene derivate
(a) Graphene oxide and (b) Reduced graphene oxide.

From the literature, it is observed that only a small amount of investigation has been conducted to date for the production of GO and rGO reinforced metal matrix composites relative to other composites [31]. Figure 2(a) shows the number of graphene related publications per year, from which it can be noted that there is a gradual increase in research publications since its discovery in the year 2004. It can be noted that 84.57% of articles out of total number of articles published were original research articles. Figure 2 (b) shows the percentage breakdown of published papers in terms of filed explored, in which only 1.67% of the work contributed towards all the physical, chemical, metallurgical and engineering aspects of the composites produced from graphene and its derivatives. There is still a long way to go in area of MMCs to develop a feasible process to produce and distribute these reinforcements in matrix homogenously. The current experimental focus from researchers internationally is to develop graphene reinforced aluminium MMCs through powder metallurgical or severe plastic deformation routes.

*ORCID ID: 0000-0003-2047-5807
E-mail: Sumsun.naher.1@city.ac.uk

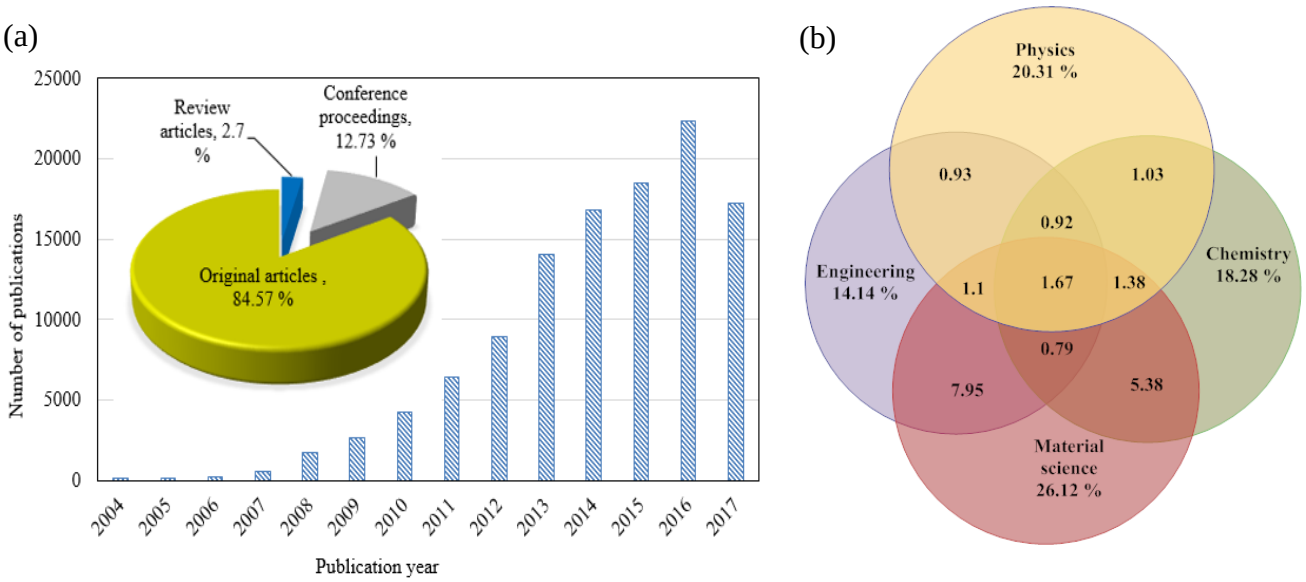

Figure 2: Research articles on graphene

(a) Number of publications corresponding to publishing year and (b) percentage breakdown of publications.

Rashad et al. [26] have successfully fabricated aluminium matrix composite reinforced with graphene nano platelets (GNP) through semi powder metallurgical route. It was reported that, the high specific area and 2-D structure of graphene increased tensile strength of the composite to nearly 11.1% with the addition of 0.3 wt% GNP's to aluminium. Stephen et al. [27] fabricated graphene–aluminium nano composites through ball milling, hot isostatic pressing and extrusion. It was reported that the tensile strength of the Al matrix composite can be increase up to 12% by using multi walled CNT's as reinforcement. Boostani et al. [29] have reported that graphene sheets as reinforcement facilitates the strengthening of Al matrix composites exceptionally, by using thermally activated dislocation and pinning the SiC nano composites to the matrix. Hwang et al. [32] demonstrated the use of rGO as reinforcement in MMC's to enhance the mechanical properties through molecular level mixing process. It was reported that elastic modulus and yield strength can be increased to 30% and 80% respectively by reinforcing Cu matrix composite with 2.5 vol% rGO. Li et al. [33] achieved uniform distribution of rGO in Al matrix through electro static interactions between the rGO and Al flakes. It was reported that, elastic modulus and hardness increased to 18% and 17% respectively, by reinforcing Al with 0.3 wt% of rGO. Shin et al. [34] have successfully fabricated aluminium alloy 2024 composites reinforced with few layer graphene using high energy ball milling followed by hot rolling. The study acknowledged that tensile strength multiplied to twice with the addition of 0.7 vol% of few layer graphene, which was a significant rise in tensile strength compared to pristine aluminium. Yolshina et al. [35] have reported a novel method of fabricating aluminium graphene metallic composites, which includes mixing of molten metal and carbon in alkali media. It was reported that the addition of 2 wt% of graphene sheets leads to nearly two times increase in hardness, strength and ductility of aluminium. Most of the research work carried out in

*ORCID ID: 0000-0003-2047-5807
E-mail: Sumsun.naher.1@city.ac.uk

the area of graphene reinforced Al matrix composite have reported the variation of properties with respect to the wt% of graphene reinforcement by reducing GO. However, from the literature it can be noted that, researchers have successfully fabricated Al matrix composites reinforced with CNTs and graphene through powder metallurgical route and reported dispersion of reinforcement in the matrix material with no disruption to the band structure. In the present study reduction steps were avoided in order to explore the potential of GO as reinforcement or Al matrix composites.

In this study, powder metallurgical technique has been used to synthesize an Al matrix composite reinforced with GO. The Al/GO composite was produced through a pressure less sintering in a horizontal tube furnace. The technique has given good results for rGO and GNS reinforced Al matrix composite in earlier studies performed by the research group [36][28]. In present research work a new solvents Isopropylalcohol (IPA) and acetone were used with a new high compaction pressure of 595 MPa and different weight percentages (0.05, 0.1 and 0.2 wt %) of reinforcement with a view to achieving improved mixing of the GO/water colloid with the Al powder to produce Al/GO composites. A magnetic stirring process was used to disperse GO in the matrix phase and the effect of wt% of GO reinforcement on microstructure and mechanical properties are investigated.

2 EXPERIMENTAL PROCEDURE

2.1 Specimen preparation

Aluminium powder with 99.9% purity of 35 µm particle size bought from East coast fiber glass suppliers was used as a matrix material and GO water dispersion (4 mg/ml) bought from Graphenea, Spain was used to produce GO reinforced aluminium matrix composites. As received Al powder was mixed with two different solvents IPA and acetone in the proportions of 200 ml of solvent for 5 g of Al for 15 minutes using magnetic stirrer. GO aqueous dispersion was sonicated for 15 minutes and added drop by drop to the Al/IPA and Al/Acetone solutions. After several iterations at different stirring times based on the wt% of GO, IPA was considered a better solvent than acetone. IPA was seen to provide a better dispersion of particles, shown in Figure 3(a). The stirring time was increased based on increased weight percentage reinforcement. The stirring times for 0.05 wt% (0.07 vol%), 0.1 wt% (0.14 vol%) and 0.2wt% (0.25 vol%) were 1, 3, and 6 hours respectively. For 0.05wt% of GO with 1 hour stirring time the clear solution achieved at the top of the beaker is shown in Figure 3(b). The solution obtained was then vacuum filtered and dried in argon atmosphere at 100°C to remove the traces of IPA. By visual inspection of the filter papers, the absence of dark brown colour was evident that GO was residing on the Al particles, shown in Figure 3(c).

*ORCID ID: 0000-0003-2047-5807
E-mail: Sumsun.naher.1@city.ac.uk

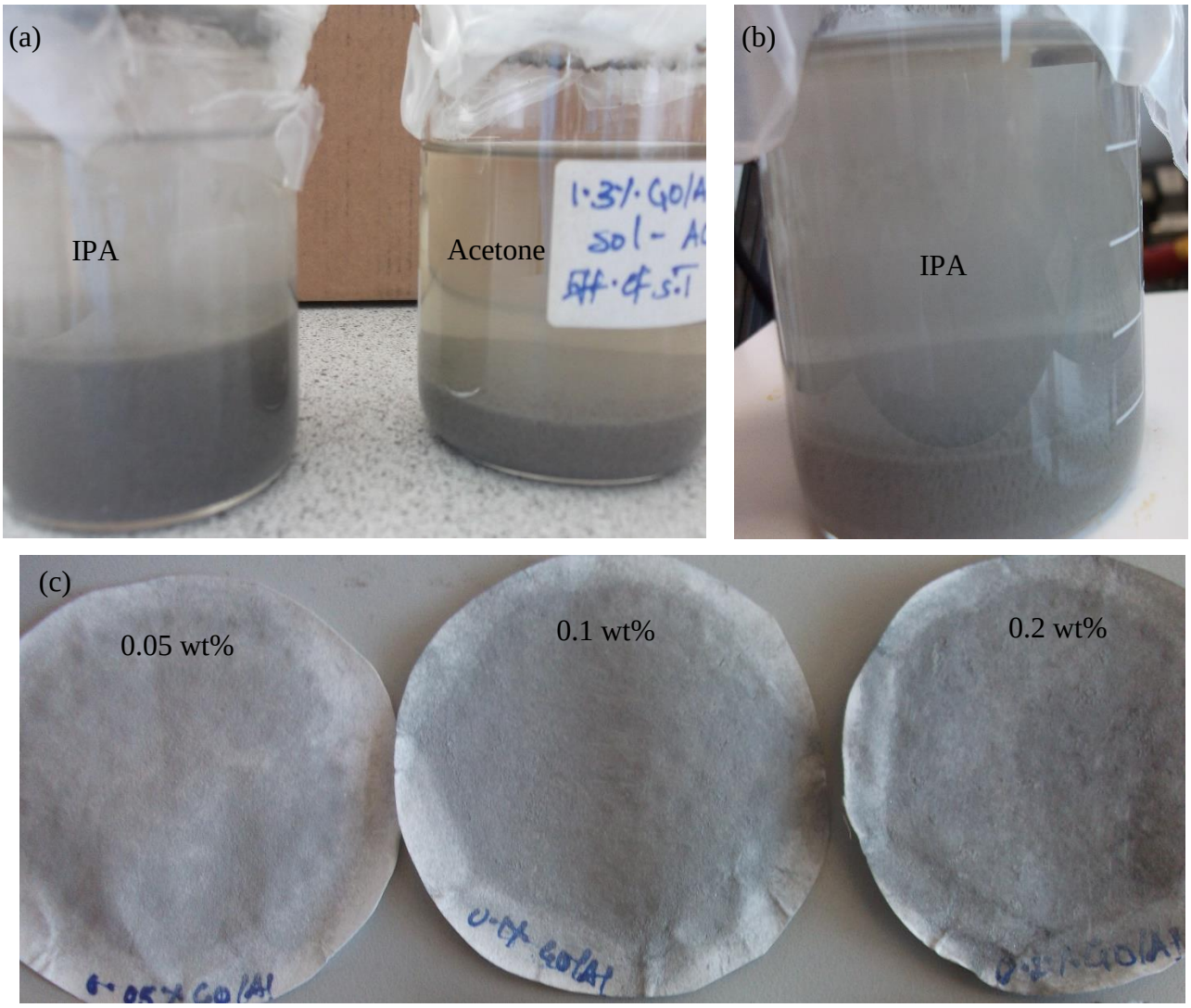

Figure 3: Visual inspection of (a) Comparison of Al/GO/IPA and Al/GO/Acetone solutions (b) 0.05 wt% of Al/GO/IPA solution after 1hour of stirring (c) Visual inspection of filter papers after filtering Al/GO/IPA solution.

A series of specimens were prepared for further characterization of Al/GO composite. Sample powders weight of 0.5g were cold compacted in evacuble pillet dies with an ATLAS 40T press. Specimens of dimensions 20 mm diameter and 0.5 mm thickness were obtained. The schematic representation of sequential steps involved in the preparation of Al/GO composite is shown in Figure 4. Before that the die surfaces were coated with rhombic boron nitride powder, which acts as a lubricant for specimen removal. The green samples were then sintered in horizontal tube furnace in argon atmosphere to 88% of melting temperature of Al i.e, 600°C [27] at dwell period of 4 hours, shown in Figure 5.

*ORCID ID: 0000-0003-2047-5807
E-mail: Sumsun.naher.1@city.ac.uk

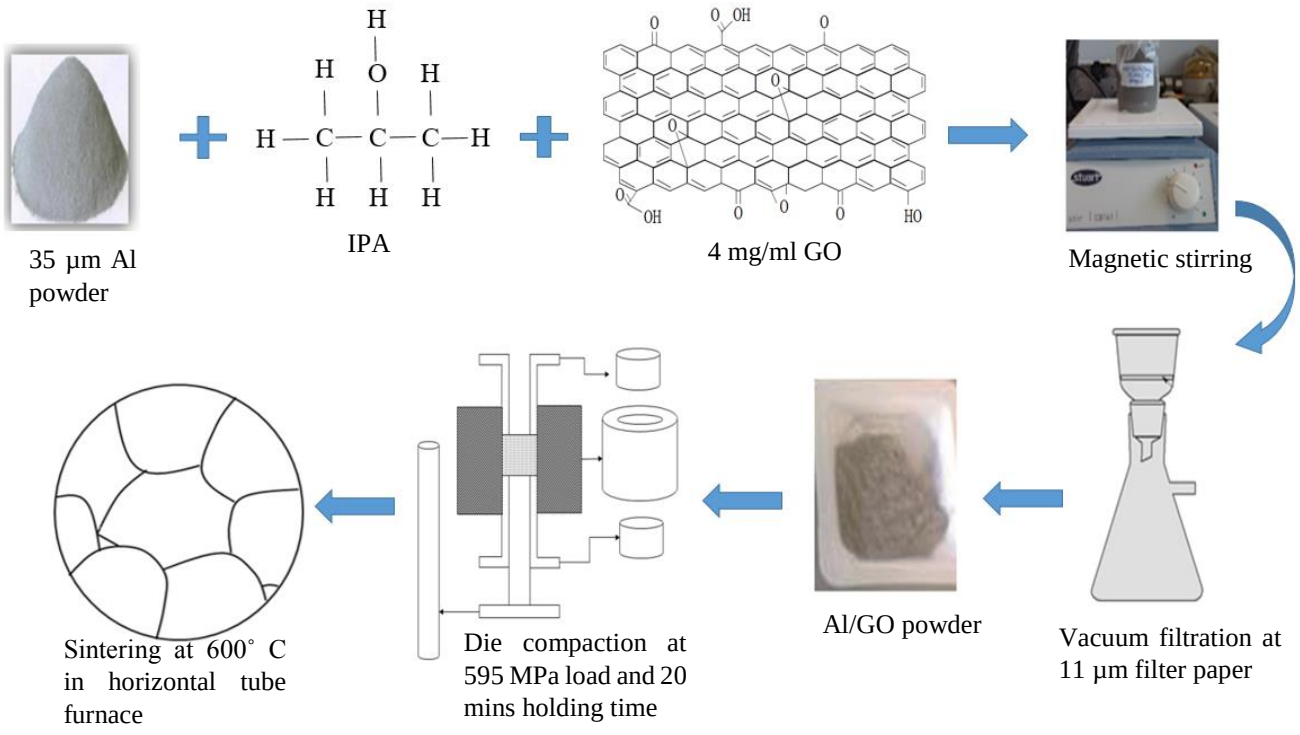

Figure 4: Schematic representation of Al/GO powder and composite preparation.

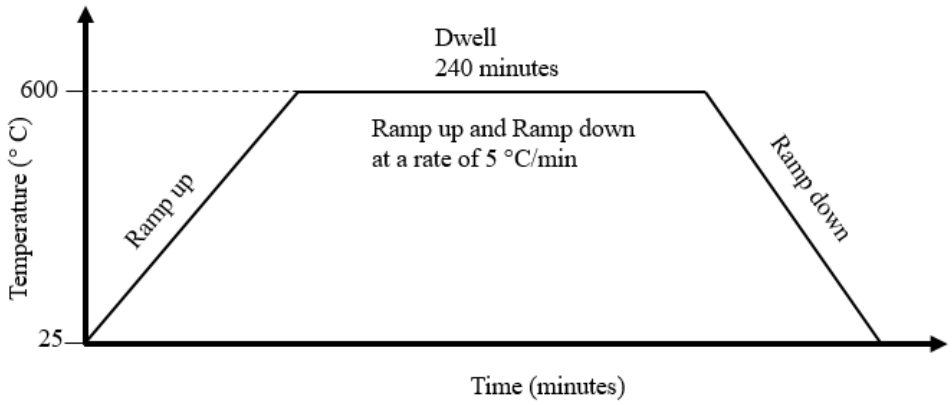

Figure 5: Sintering profile for composite preparation.

2.2 Characterization

Scanning Electron Microscopy (SEM) images obtained from EVOLS15, Carl Zeisis at 1.0 kV and 15.0 kV were used to investigate the particle morphologies of as received Al, processed Al/GO powders and Al/GO composites. Energy Dispersive X-ray Spectroscopy (EDX) equipped to SEM was used to scan the composites to analyse elements and the percentage of elements present at random locations of the composites.

Pristine Al and various vol% of Al/GO samples were analysed using Bruker D8 advance X-ray diffractometer to identify the phases of a crystalline material and to check whether the carbide is formed

*ORCID ID: 0000-0003-2047-5807
E-mail: Sumsun.naher.1@city.ac.uk

during the consolidation. For all the samples scan speed of 0.1°/min was used for Z-scan from 0.99 to 1.99, Chi-scan from -3 to 3, Phi-scan from -180° to +180° and 2θ-scan from -5 to 90.

Micro Raman spectroscopy was performed to study the Raman spectra were noted at room temperature using a Jobin Yvon Horiba Lab RAM 800 spectrometer equipped with Ar+ laser with web length of 488 nm. The specimens analysed included different vol% of Al/GO composites at multiple locations.

Vickers hardness tests were performed by Leitz micro hardness tester, applying constant load of 981 mg and load holding time of 20 sec. A minimum of 4 data points at random locations were measured and measured the average value with standard deviation for each composition of the material. This process was repeated for 3 samples each at 0.05 wt%, 0.1 wt% and 0.2 wt% Al/GO composites. Test was performed at standard laboratory conditions.

Pure Al and Al/GO samples were examined using indentation or puncture test using Zwick Roell, UK with load limit of 5 kN at indentation rate of 1mm/min. The test was carried out in standard laboratory conditions, temperature of 23±2 °C and relative humidity of 50±5 %. This procedure was repeated for 3 samples each at 0.05 wt%, 0.1 wt% and 0.2 wt% Al/GO composites. The stresses acting on the specimens were calculated based on the force recorded by the load cell using equations 1 to 3 [37][38].

$$\sigma_r = \frac{3P}{4\pi t^2}(1+\vartheta)\log R/x \tag{1}$$

$$\sigma_t = \frac{3P}{4\pi t^2}\left((1+\vartheta)\log R/x + (1-\vartheta)\right) \tag{2}$$

$$y = \frac{3PR^2}{4\pi E t^3}(3+\vartheta)(1-\vartheta) \tag{3}$$

Where,

y is deflection in center, P is load in center, R is radius of the specimen, t is thickness of specimen, E is Young's modulus, ϑ is Poisson's ratio, σ_r is radial stress, σ_t is tangential stress, x is diameter of indenter.

3. RESULTS AND DISCUSSION

3.1 Microstructure

Figure 6 shows the SEM images of particles morphologies of pure Al and 0.05 wt%, 0.1 wt%, 0.2 wt% of Al/GO powders with optimized stirring times. For the Al/GO powders the magnified image of the particles was given in inset. It is evident from the dark black regions on the particles that GO exists on the particles, this analysis fits well with the analysis from literature [36]. The particle size of Al particles were increased from a typical size of 35 µm to 40 µm with reinforced with GO.

*ORCID ID: 0000-0003-2047-5807
E-mail: Sumsun.naher.1@city.ac.uk

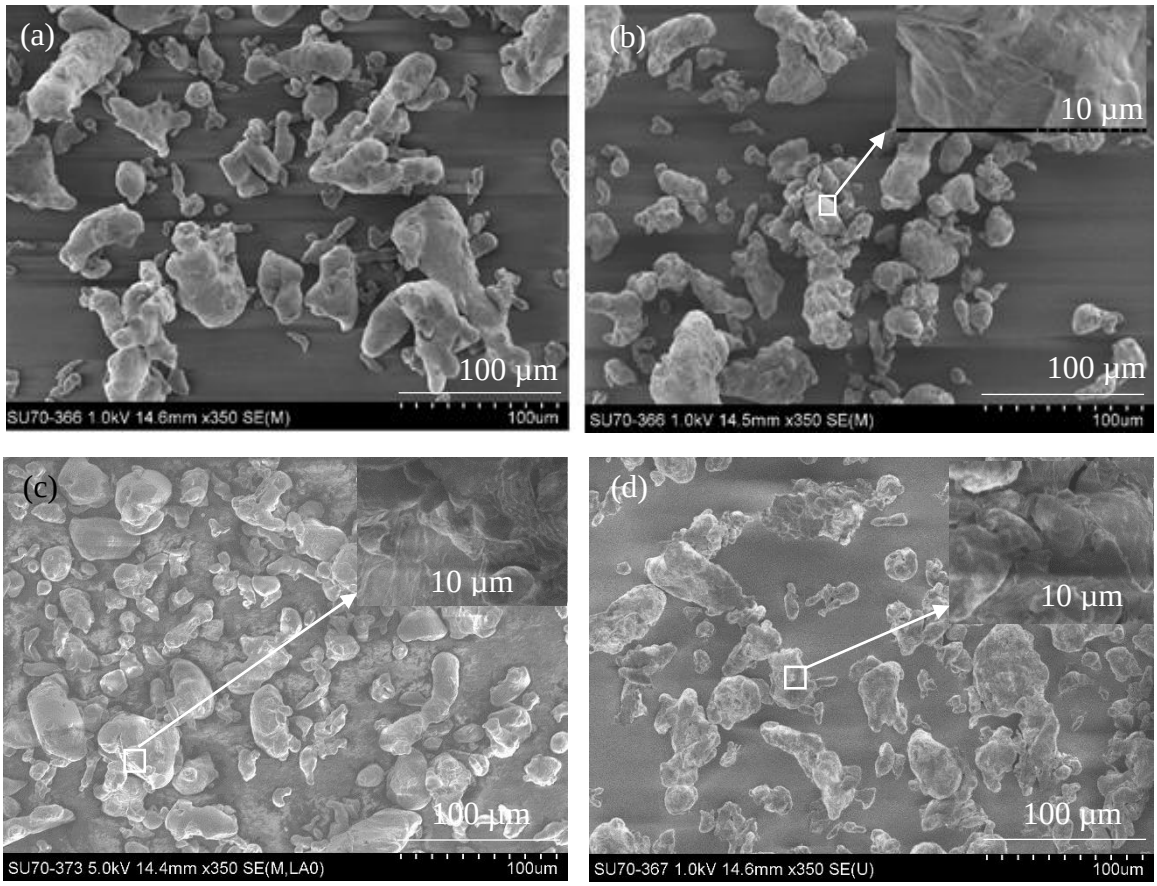

Figure 6: (a) Particle morphology of 35µm Al powder (b) 0.05 wt% of Al/GO powder (c) 0.1 wt% of Al/GO powder (d) 0.2 wt% of Al/GO powder.

Typical SEM images and EDX spectra of 0.05 wt %, 0.1 wt% and 0.2 wt% of GO in Al matrix are shown in Figure 7. The SEM images show the GO nano particles are dispersed around the aluminium matrix which is required to improve the mechanical properties of GO reinforced aluminium matrix composite. It is obvious that there will be pores formation inside the composite structure prepared by powder metallurgy if there is lack of sintering process such as temperature, wettability of the matrix and particles size and compression pressure. The SEM results show some porosity and grain boundary like structure which might due to one of the factors mentioned above. For further investigation, the specimens were analysed on EDX to study the presence of different elements in the composites, in parallel with the study of homogeneous distribution of GO, shown in Figures 7(b), 7(d) and 7(e). It can be noted that the aluminium, carbon and oxygen peaks of these samples indicate that the GO is dispersed in to the Al matrix. There was no evidence found for aluminum carbide (Al_4C_3) as reported in other reported work [27]. It can also be noted from the SEM images that the porosity increased with increase in wt% of GO reinforcement as with an increase in nano particle concentration, increased agglomeration would be expected.

*ORCID ID: 0000-0003-2047-5807
E-mail: Sumsun.naher.1@city.ac.uk

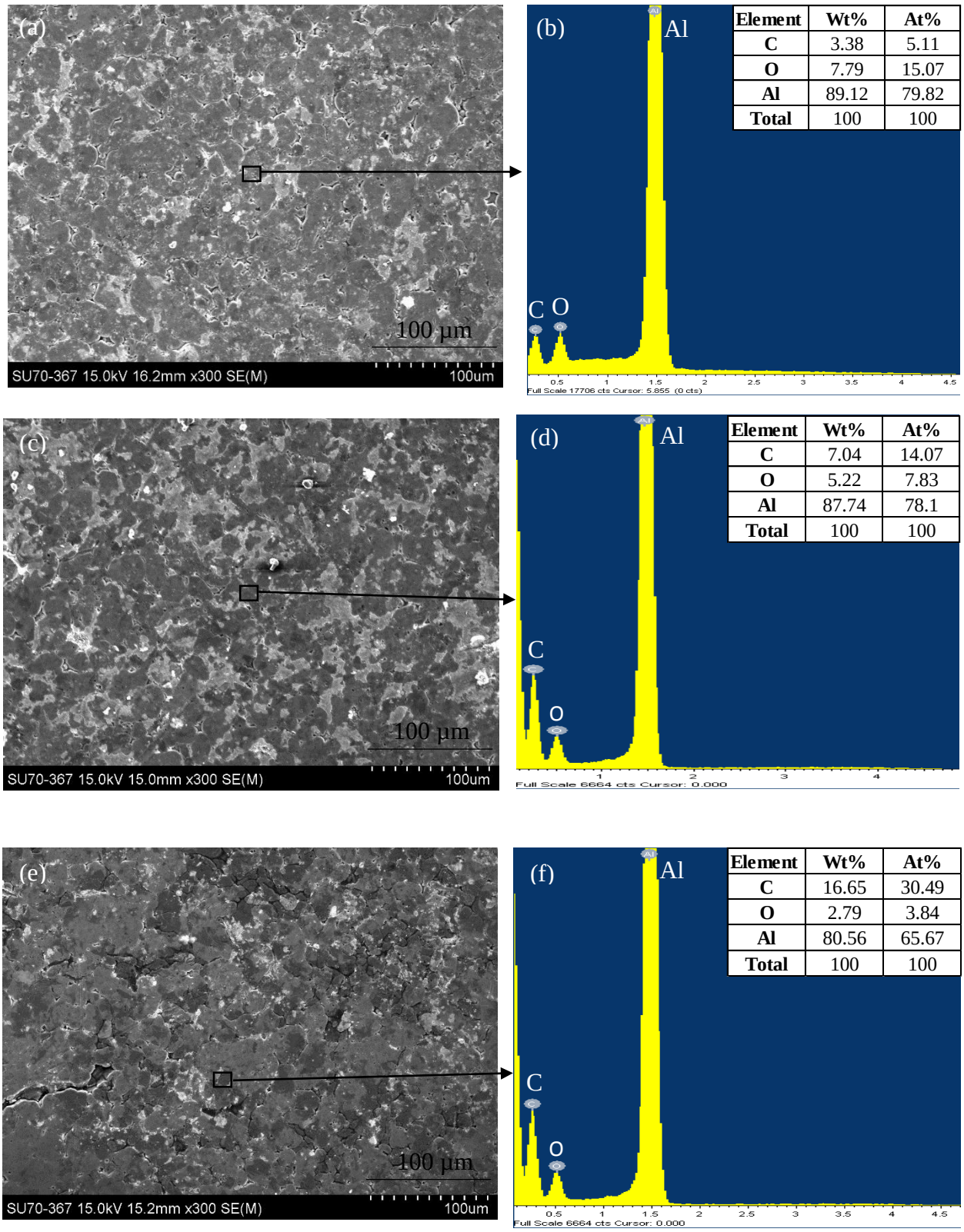

Element	Wt%	At%
C	3.38	5.11
O	7.79	15.07
Al	89.12	79.82
Total	100	100

Element	Wt%	At%
C	7.04	14.07
O	5.22	7.83
Al	87.74	78.1
Total	100	100

Element	Wt%	At%
C	16.65	30.49
O	2.79	3.84
Al	80.56	65.67
Total	100	100

Figure 7: (a) SEM image of 0.05 wt% Al/GO composite (b) EDX spectrum of 0.05 wt% Al/GO (c) SEM image of 0.1 wt% Al/GO composite (d) EDX spectrum of 0.1 wt% Al/GO (e) SEM image of 0.2 wt% Al/GO composite (f) EDX spectrum of 0.2 wt% Al/GO.

*ORCID ID: 0000-0003-2047-5807
E-mail: Sumsun.naher.1@city.ac.uk

The structural changes and crystalline phase evaluation of the sintered pure Al and Al/GO composites as characterised in X-ray diffraction (XRD) are shown in Figure 8. The phases were calculated based on Bragg's law and 2θ values. The various crystalline phases of Al were observed at 38.6° (111), 45° (200), 65.3° (220), 78.7° (311) and 82.7° (222) of 2θ. The crystalline phases matches well with the phases that were observed by Jing et al. [36]. It can be noted that the crystalline forms were not affected by the sintering process. There was no visible evidence of broadening of peaks as the wt% of GO increased. It can be noted that the internal stresses were relieved during the sintering process. However, the presence of aluminium oxide (Al_2O_3) is still inevitable. While these carbides could theoretically have formed at the sintering temperatures of 600° [39], there was no evidence of Al_4C_3 peaks in the XRD results. Carbides typically will negatively effect the overall strength of the composite [27]. Carbide formation is most likely to exist at the defects in the graphitic planes, at composite edges and amorphous carbon coatings below the melting point of aluminium [40].

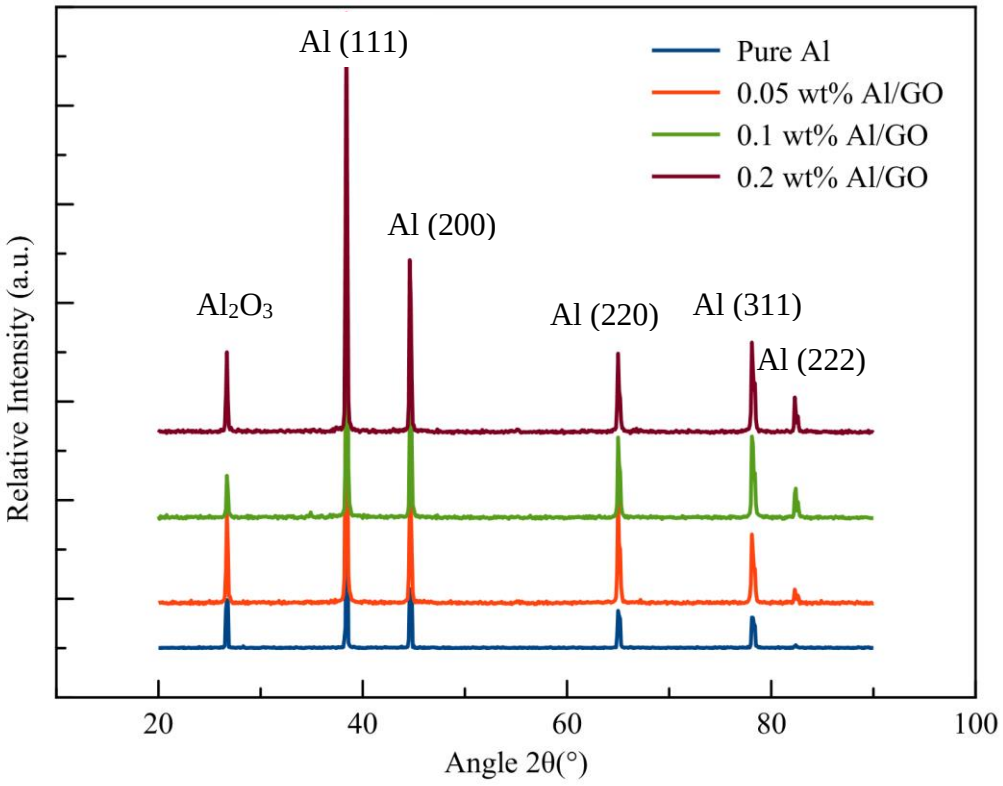

Figure 8: XRD spectra of pure Al, 0.05 wt%, 0.1 wt% and 0.2 wt% Al/GO composites.

Micro Raman spectroscopy was used to analyse the evaluation of graphene structures during the composite processing and spectra is related to the quality of graphene. The samples used for the analysis are 0.05 wt%, 0.1 wt% and 0.2 wt% of Al/GO composites at three locations for each sample. The Raman peaks recorded were fitted with the Lorenz function to obtain the wavenumber and Raman intensity and these results were summarized in Table 1(a), Table 1(b) and Table 1(c). Three major peaks of D-band,

*ORCID ID: 0000-0003-2047-5807
E-mail: Sumsun.naher.1@city.ac.uk

G-band and 2D-band were observed in the Raman spectrum and indicates that there is no alteration in chemical structure of graphene in Al matrix. The G-band is related to the intrinsic vibration modes of graphene crystal, D-band is the peak related to the disorders in GO used, presence of sp^3 defects can also be evaluated whereas 2D- band is the overtone of D-band which usually is smaller in intensity than G and D-bands. The ratio of intensities of D-band and G-band (I_D/I_G) used to evaluate the disorderness and defect density of the graphene. Figure 9(a) shows the Raman spectra of 0.05 wt% Al/GO composite at three random locations, it can be noted from the spectra that the G-band peak was recorded at approximately 1604 cm^{-1}. The ratio of intensities varies from location to location which implies to the need for the improved homogeneity in GO distribution over the composite and the similar trends were observed for 0.1 wt% shown in Figure 9(b) and 0.2 wt% show in Figure 9(c) of Al/GO composites. The uniform distribution of reinforcement of in matrix material strongly depends on the stirring speed and time [41] from the observations noted from the intensities of Raman spectra implies to the need of re-evaluating the process parameters. By comparison of Raman spectra of 0.05 wt%, 0.1 wt% and 0.2 wt% Al/GO composites, the I_D/I_G ratio varies with increase in wt% of GO reinforcement. The ratio was decreased from 0.05 wt% to 0.1 wt% but increased from 0.1 wt% to 0.2 wt%. This resulted due to the increase in physical force applied on particles with increase in stirring times that contributed to the increase in more defects in disorderness in the graphene clusters [42].

The number of graphene layers decreases as the ratio of I_G/I_{2D} ratio decreases [43]. It can be noted from the Raman data that with increase in wt% of GO reinforcement the I_D/I_G ration increased which implies that the number of graphene layers increased from 0.69 to 0.89 (monolayer of graphene has a I_D/I_G value of 0.28 [44]) which is due to the agglomeration of GO reinforcement. The agglomeration is caused due to the insufficient amount of force applied during stirring that failed to separate the graphene layers from each other. The stress experienced by the composites can be evaluated using the G-band peak positions (ω_G). The vibration frequency of the G-band changes due to the change in interatomic distances of graphene when graphene undergoes strain this will result in shift in wavenumbers. This means the shift of wavenumber will be higher if graphene experiences more strain. In the present study, the wavenumber of Al/GO is more than the as received GO which is due to the increase in residual compressive stresses with reduction in interatomic distances in graphene. Meanwhile, approximately 0.2-0.3 variation of wavenumbers with increase in wt% of GO reinforcement indicates that the stress experienced by the GO is almost negligible [45]. However, the peak at 850 cm^{-1} correspond to Al_4C_3 was not observed in all samples indicates that the composites were made with Al and GO [46]. XRD results also confirmed that there is no Al_4C_3 phase inside the Al/GO composite.

*ORCID ID: 0000-0003-2047-5807
E-mail: Sumsun.naher.1@city.ac.uk

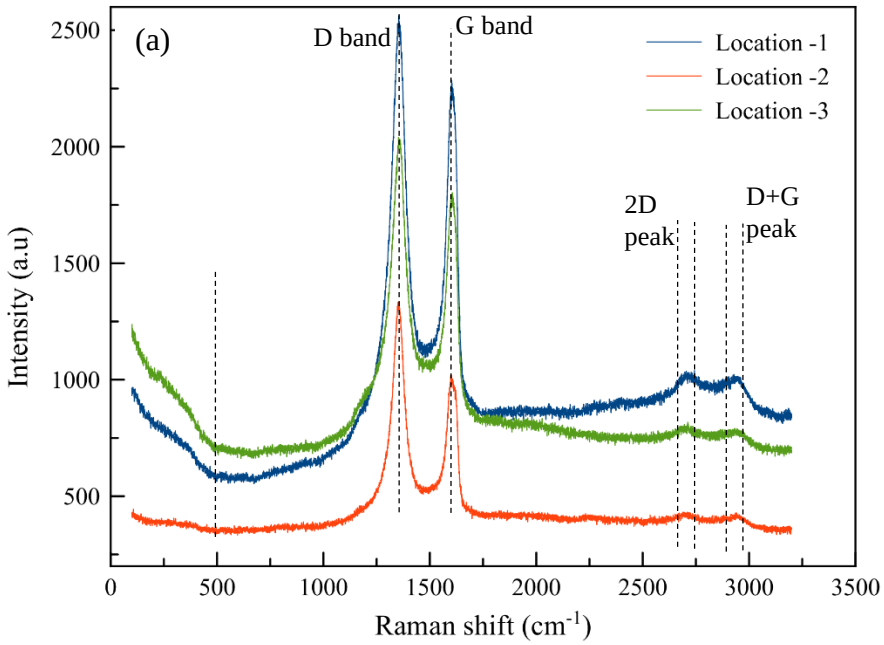

Figure 9(a): Recorded micro Raman for 0.05 wt% Al/GO composite.

Table 1(a): Raman data of the 0.05 wt% Al/GO composite at random locations.

Material	I_D/I_G	I_G/I_{2D}	ω_G (cm^{-1})
As received GO	1.07	0.69	1507.7
Location - 1	1.147	0.72	1606.07
Location – 2	1.311	0.7	1598.92
Location – 3	1.137	0.69	1600.23

*ORCID ID: 0000-0003-2047-5807
E-mail: Sumsun.naher.1@city.ac.uk

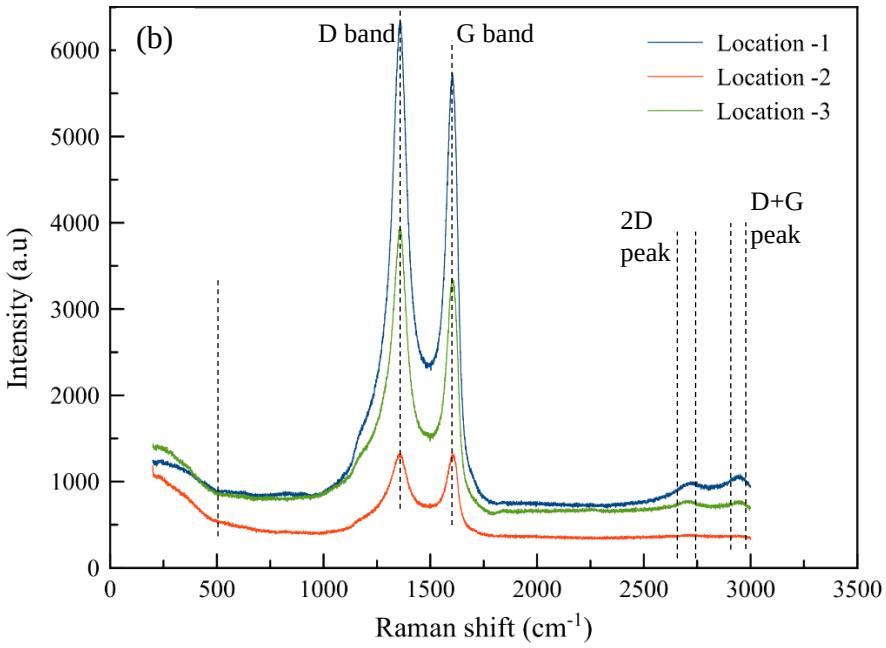

Figure 9(b): Recorded micro Raman for 0.1wt% Al/GO composite.

Table 1(b): Raman data of the 0.1 wt% Al/GO composite at random locations.

Material	I_D/I_G	I_G/I_{2D}	ω_G (cm^{-1})
As received GO	1.07	0.69	1507.7
Location - 1	1.1042	0.78	1604.23
Location – 2	1.00417	0.74	1604.49
Location – 3	1.184	0.76	1608.72

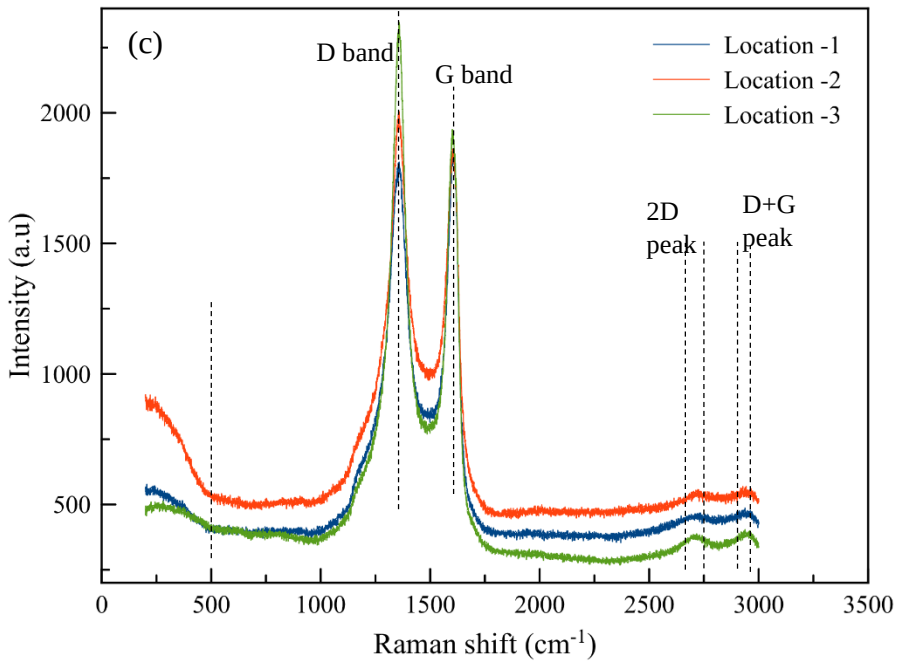

*ORCID ID: 0000-0003-2047-5807
E-mail: Sumsun.naher.1@city.ac.uk

Figure 9(c): Recorded micro Raman for 0.2 wt% Al/GO composite.

Table 1(c): Raman data of the 0.2 wt% Al/GO composite at random locations.

Material	I_D/I_G	I_G/I_{2D}	ω_G (cm^{-1})
As received GO	1.07	0.69	1507.7
Location - 1	1.0064	0.82	1606.87
Location – 2	1.087	0.89	1606.08
Location – 3	1.211	0.869	1605.02

3.2 Mechanical properties

3.2.1 Vickers hardness

The hardness of a material as a surface rather than a bulk property is dependent on the atomic structure and grain size near the surface of the material. Figure 10 shows Vickers micro hardness of the sintered pure Al and Al/GO composites. The results show that the hardness value increased with increasing the GO percentage in the composite due to the formation of more refined and compacted microstructure. From these results it is noted that there was a 16%, 23% and 29% of hardness increase with 0.05wt%, 0.1wt% and 0.2 wt% of GO reinforcement respectively. However, this increase was less compared to that found in other reported work for Al/GO composites [36][47]. The hardness can be further increased by avoiding agglomeration and achieving a uniform distribution of GO throughout the matrix which would be expected to result in more uniform alteration of mechanical properties and increase in hardness.

*ORCID ID: 0000-0003-2047-5807
E-mail: Sumsun.naher.1@city.ac.uk

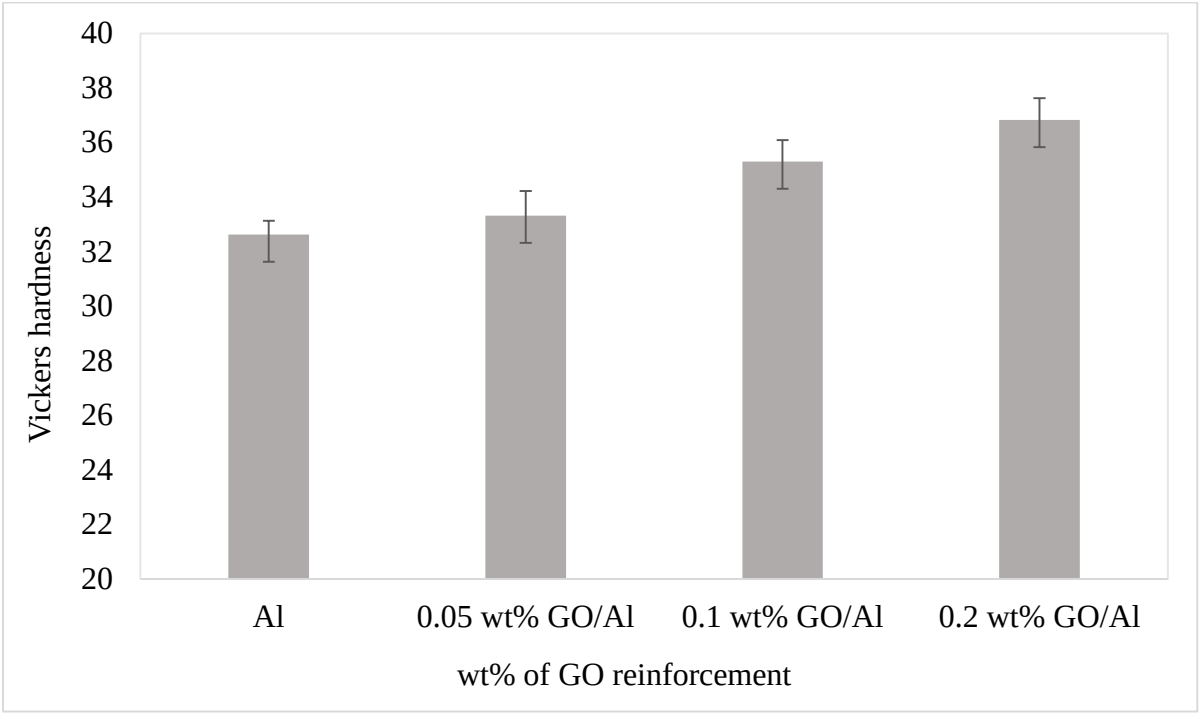

Figure 10: Micro Vickers hardness values measured for different wt% of Al/GO composites, n=12 and confidence interval of 95%.

3.2.2 Indentation test

The strength of the material is dependent on the grain structures where weak grain boundaries or grain structures are more prone to cracking which leads to failure of the material. The indentation compression load was applied centrally on the specimens of pure Al, 0.5 wt%, 0.1 wt% and 0.2 wt% of GO reinforced composites. Pure Al sample shows ductile failure and the 0.05 wt% and 0.1 wt% Al/GO composites exhibited ductile shear failure, see Figure 11. Whereas brittle failure with grain cleavage was observed in 0.2 wt% of Al/GO composite. It can be noted from Figure 12 that the stress generated in the material during loading is higher in the tangential direction than in the radial direction. The decrease in stress with increasing wt% GO is opposite to the trend that was observed with hardness values where the hardness increased with increasing wt% GO.

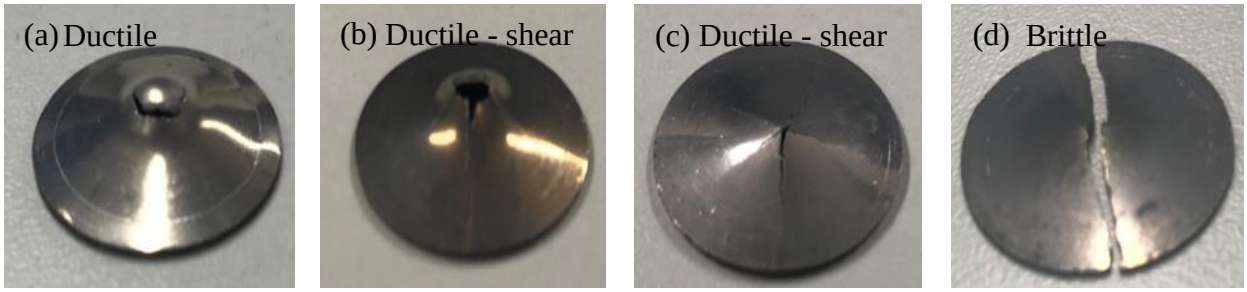

Figure 11: Pictures of the tested indentation samples of (a) pure Al, (b) 0.05 wt% Al/GO, (c) 0.1 wt% Al/GO, and (d) 0.2 wt% Al/GO.

*ORCID ID: 0000-0003-2047-5807
E-mail: Sumsun.naher.1@city.ac.uk

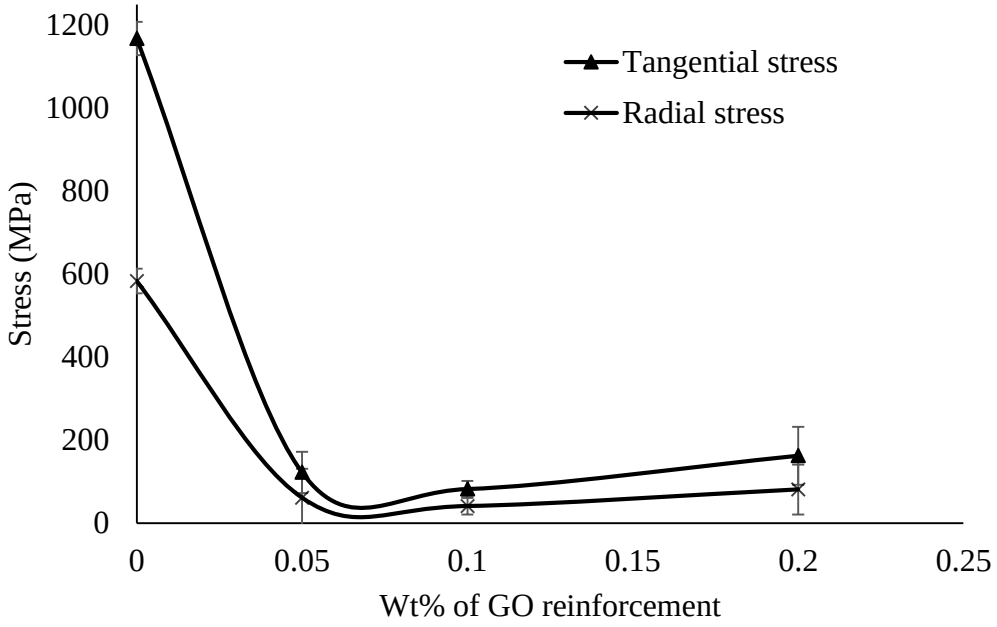

Figure 12: Variation of tangential and radial stresses for the various wt% of GO reinforcement, n=12 and confidence interval of 95%.

Figure 13(a) sows the fracture surface morphology of the samples produced from the pure Al pellets. A semi-spherical damage area was observed and the failure occurred in ductile mode showing necking and no significant strain hardening. The fracture surface of the 0.05 wt% of Al/GO composite is shown in Figure 13(b) in which un-melted particles remained and promoted the nucleation of porosity which has led to crack propagation. Figure 13(c) shows the SEM fracture image of 0.1 wt% Al/GO composite which follows a similar trend as observed in sample 0.05 wt%. Further increase in wt% of GO reinforcement from 0.1% to 0.2% resulted in brittleness in the composite, the fracture morphology is shown in Figure 13(d). It can be noted that with the increase in wt% of reinforcement, increased cracking at the micro and macro scales resulted. These structures have promoted more stress concentration and resulted in increased crack propagation leading to the brittle nature of the composite.

*ORCID ID: 0000-0003-2047-5807
E-mail: Sumsun.naher.1@city.ac.uk

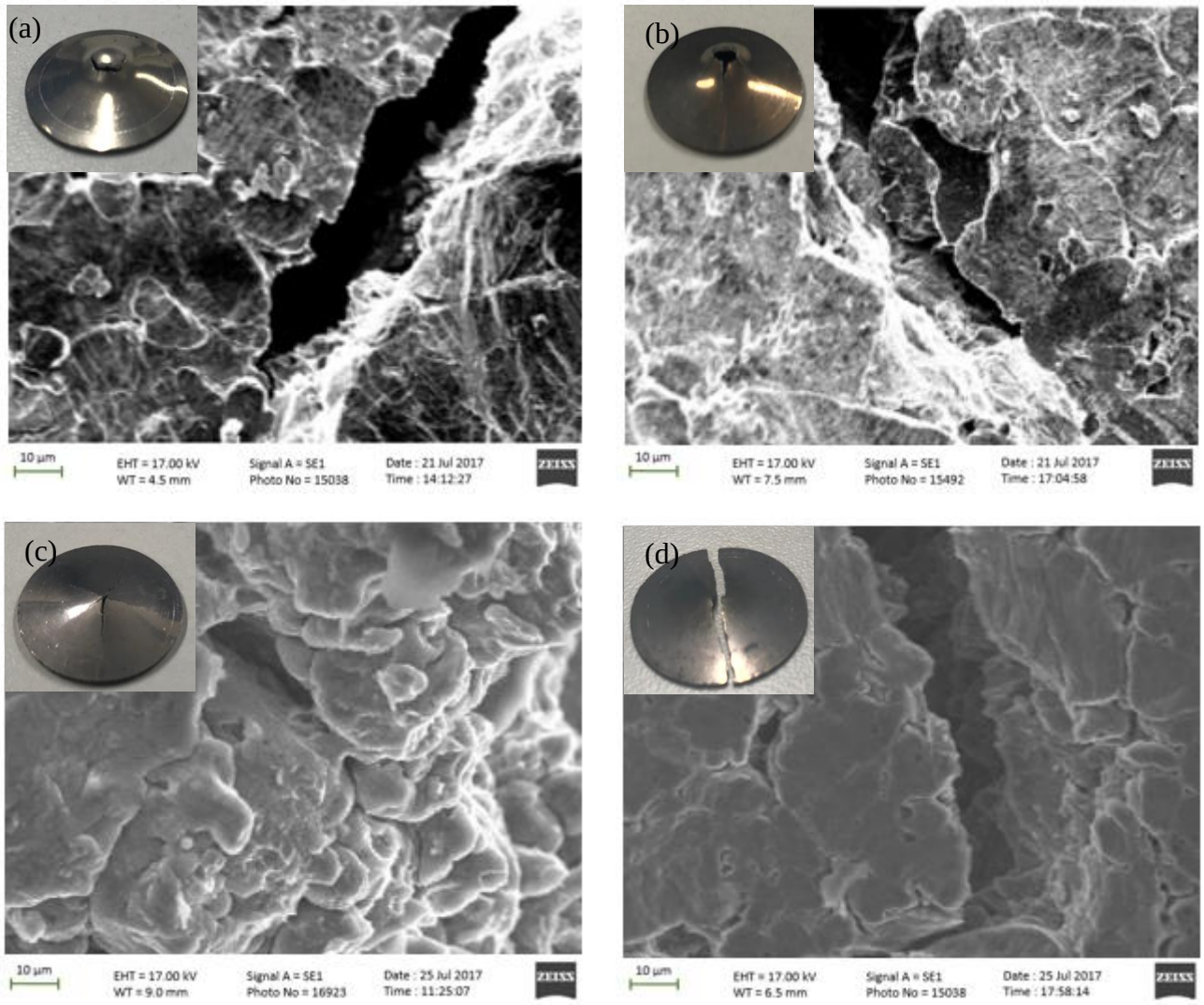

Figure 13: Fracture surface morphologies (a) Pure Al (b) 0.05 wt% Al/GO (c) 0.1 wt% Al/GO and (d) 0.2 wt% Al/GO.

Due to the high cost and unavailable manufacturing techniques, pure graphene reinforced metal matrix composites have not been reported yet. Most of the literature reports on reduced graphene oxide and also graphene nano sheets reinforced composites. The factors such as high porosity and the introduction of longitudinal alignment after manufacturing procedures limits the applications of CNT's in MMC's [48]. The dispersion of graphene in the MMC with the existing metallurgical methods is quite challenging due to the huge size differences between graphene nanosheets and metal matrix. Aluminium matrix composites have been used in flywheel enables smaller flywheels compared to polymer composites. The experimental study of Al matrix composite reinforced with GNS have shown that a tensile strength of 249 MPa can be achieved with 0.5% of graphene [47]. Further increase is theoretically possible with the more homogeneity in distribution of GNS in Al matrix. The full exfoliation of graphene into single or few layer material and good dispersion leads to the production of nanocomposites with low mass density, high

*ORCID ID: 0000-0003-2047-5807
E-mail: Sumsun.naher.1@city.ac.uk

strength and stiffness. Unlike the CNT's, which are strong in longitudinal direction, graphene is a processing material that is strong enough across it's in plane directions. GNP's has been shown in this sense to outperform CNT's in terms of enhancing mechanical properties [49]. The development of optimised experimental method is an important issue in designing graphene based composites in some applications. Numerous experimental efforts have been made to evaluate the mechanical performance of graphene and composites reinforced by graphene. Trying not only to measure the mechanical properties of graphene reinforced composite but also development of production of the reinforced composite for the use of practical applications is the motive to develop the improved methodologies [36].

4 CONCLUSIONS

The strength and stiffness of graphene reinforced metal matrix composites can lead to the production of composites with excellent mechanical properties. A successful initial optimisation of process parameters to produce graphene reinforced Al matrix composites via liquid phase mixing and powder metallurgy has been established in this paper. The need to further improve the homogeneity of the reinforcement distribution has been identified. The change of Raman peak position and intensity indicate that the residual stress inside the composite varied with process parameters such as sintering pressure, time, temperature and percentage of GO content in the composite. To achieve the optimal materials properties, it is important to optimise the process parameters such as selection of solvent, stirring time and speed, compaction pressure and sintering time, temperature. Further work will be carried out to optimisation of processing parameter for optimal Al/GO composite production. An increase of 28.64% in micro hardness was observed with 0.2 wt% of GO reinforcement. From the fracture analysis, it can be noted that it is possible to obtain the composite with high strength and ductility through the homogeneity of materials in the composite. It can be concluded that graphene reinforced aluminium can be a promising material for practical applications. In future work, the experimental method reported in this paper will be extended to different particle sizes, stirring times and wt% of reinforcement with a primary goal to achieve homogeneous distribution of reinforcement such that optimal and high repeatability of mechanical properties can be achieved.

REFERENCES

[1] Z. M. Gasem, "Fatigue crack growth behavior in powder-metallurgy 6061 aluminum alloy reinforced with submicron Al2O3 particulates," *Compos. Part B Eng.*, vol. 43, no. 8, pp. 3020–3025, 2012.

[2] L. Dyachkova and E. E. Feldshtein, "On the properties of composites based on sintered bronze with alumina additives," *Compos. Part B Eng.*, vol. 45, no. 1, pp. 239–247, 2013.

*ORCID ID: 0000-0003-2047-5807
E-mail: Sumsun.naher.1@city.ac.uk

[3] S. Rawal, “Metal-Matrix Composites for Space Applications,” *J. Miner.*, vol. 53, no. 4, pp. 14–17, 2001.

[4] Lim CS and Clegg AJ, “The production and evaluation of metal matrix composite casting produced by a pressure-assisted investment casting process,” *J. Mater. Process. Technol.*, vol. 67, pp. 13–18, 1997.

[5] R.D. Carnahan, R.F. Decker, N. Bradley, and P. Frederick, “New manufacturing process for metal matrix composite synthesis,” ASM Int., pp. 101–106, 1990.

[6] C. Balázsi *et al.*, “Development of CNT/Si3N4 composites with improved mechanical and electrical properties,” *Compos. Part B Eng.*, vol. 37, no. 6, pp. 418–424, 2006.

[7] A. Dorri Moghadam, E. Omrani, P. L. Menezes, and P. K. Rohatgi, “Mechanical and tribological properties of self-lubricating metal matrix nanocomposites reinforced by carbon nanotubes (CNTs) and graphene - A review,” *Compos. Part B Eng.*, vol. 77, pp. 402–420, 2015.

[8] M. Karbalaei Akbari, H. R. Baharvandi, and O. Mirzaee, “Fabrication of nano-sized Al2O3 reinforced casting aluminum composite focusing on preparation process of reinforcement powders and evaluation of its properties,” *Compos. Part B Eng.*, vol. 55, pp. 426–432, 2013.

[9] A. Kurun, E. Bayraktar, and H. M. Enginsoy, “Experimental and numerical study of alumina reinforced aluminum matrix composites: Processing, microstructural aspects and properties,” *Compos. Part B Eng.*, vol. 90, pp. 302–314, 2016.

[10] J. K. Chen and I. S. Huang, “Thermal properties of aluminum-graphite composites by powder metallurgy,” *Compos. Part B Eng.*, vol. 44, no. 1, pp. 698–703, 2013.

[11] F. Gardea and D. C. Lagoudas, “Characterization of electrical and thermal properties of carbon nanotube/epoxy composites,” *Compos. Part B Eng.*, vol. 56, pp. 611–620, 2014.

[12] B. L. Dasari, J. M. Nouri, D. Brabazon, and S. Naher, “Graphene and derivatives – Synthesis techniques, properties and their energy applications,” *Energy*, vol. 140, pp. 766–778, 2017.

[13] A. Baradeswaran and A. E. Perumal, “Wear and mechanical characteristics of Al 7075/graphite composites,” *Compos. Part B Eng.*, vol. 56, pp. 472–476, 2014.

[14] R. Barretta, M. Brčić, M. Čanađija, R. Luciano, and F. Marotti de Sciarra, “Application of gradient elasticity to armchair carbon nanotubes: Size effects and constitutive parameters assessment,” *Eur. J. Mech. A/Solids*, vol. 65, pp. 1–13, 2017.

[15] A. Apuzzo, R. Barretta, M. Canadija, L. Feo, R. Luciano, and F. Marotti de Sciarra, “A closed-

*ORCID ID: 0000-0003-2047-5807
E-mail: Sumsun.naher.1@city.ac.uk

form model for torsion of nanobeams with an enhanced nonlocal formulation," *Compos. Part B Eng.*, vol. 108, pp. 315–324, 2017.

[16] R. Barretta, L. Feo, R. Luciano, and F. Marotti De Sciarra, "Application of an enhanced version of the Eringen differential model to nanotechnology," *Compos. Part B Eng.*, vol. 96, pp. 274–280, 2016.

[17] R. Barretta, L. Feo, and R. Luciano, "Torsion of functionally graded nonlocal viscoelastic circular nanobeams," *Compos. Part B Eng.*, vol. 72, pp. 217–222, 2015.

[18] G. Romano and R. Barretta, "Stress-driven versus strain-driven nonlocal integral model for elastic nano-beams," *Compos. Part B Eng.*, vol. 114, pp. 184–188, 2017.

[19] R. Barretta, M. Diaco, L. Feo, R. Luciano, F. M. de Sciarra, and R. Penna, "Stress-driven integral elastic theory for torsion of nano-beams," *Mech. Res. Commun.*, vol. 87, pp. 35–41, 2017.

[20] R. Barretta, L. Feo, R. Luciano, F. Marotti de Sciarra, and R. Penna, "Functionally graded Timoshenko nanobeams: A novel nonlocal gradient formulation," *Compos. Part B Eng.*, vol. 100, pp. 208–219, 2016.

[21] A. Apuzzo, R. Barretta, R. Luciano, F. Marotti de Sciarra, and R. Penna, "Free vibrations of Bernoulli-Euler nano-beams by the stress-driven nonlocal integral model," *Compos. Part B Eng.*, vol. 123, pp. 105–111, 2017.

[22] A. M. K. Esawi, K. Morsi, A. Sayed, M. Taher, and S. Lanka, "Effect of carbon nanotube (CNT) content on the mechanical properties of CNT-reinforced aluminium composites," *Compos. Sci. Technol.*, vol. 70, no. 16, pp. 2237–2241, 2010.

[23] M. M. H. Bastwros, A. M. K. Esawi, and A. Wifi, "Friction and wear behavior of Al-CNT composites," *Wear*, vol. 307, no. 1–2, pp. 164–173, 2013.

[24] J. Liao and M. J. Tan, "Mixing of carbon nanotubes (CNTs) and aluminum powder for powder metallurgy use," *Powder Technol.*, vol. 208, no. 1, pp. 42–48, 2011.

[25] M. Bastwros *et al.*, "Effect of ball milling on graphene reinforced Al6061 composite fabricated by semi-solid sintering," *Compos. Part B Eng.*, vol. 60, pp. 111–118, 2014.

[26] M. Rashad, F. Pan, A. Tang, and M. Asif, "Effect of Graphene Nanoplatelets addition on mechanical properties of pure aluminum using a semi-powder method," *Prog. Nat. Sci. Mater. Int.*, vol. 24, no. 2, pp. 101–108, 2014.

*ORCID ID: 0000-0003-2047-5807
E-mail: Sumsun.naher.1@city.ac.uk

[27] S. F. Bartolucci *et al.*, “Graphene–aluminum nanocomposites,” *Mater. Sci. Eng. A*, vol. 528, no. 27, pp. 7933–7937, 2011.

[28] J. Liu et al., “Powder processing methodology for production of graphene oxide reinforced aluminium matrix composites, Advances in Materials and Processing Technologies, vol. 2(4), pp. 437-450, 2016.

[29] A. Fadavi Boostani *et al.*, “Strengthening mechanisms of graphene sheets in aluminium matrix nanocomposites,” *Mater. Des.*, vol. 88, pp. 983–989, 2015.

[30] H. G. P. Kumar and M. A. Xavior, “Graphene Reinforced Metal Matrix Composite (GRMMC): A Review,” *Procedia Eng.*, vol. 97, pp. 1033–1040, 2014.

[31] V. Dhand, K. Y. Rhee, H. Ju Kim, and D. Ho Jung, “A Comprehensive Review of Graphene Nanocomposites: Research Status and Trends,” *J. Nanomater.*, vol. 2013, pp. 1–14, 2013.

[32] J. Hwang *et al.*, “Enhanced Mechanical Properties of Graphene/Copper Nanocomposites Using a Molecular-Level Mixing Process,” *Adv. Mater.*, vol. 25, no. 46, pp. 6724–6729, 2013.

[33] Z. Li *et al.*, “Uniform dispersion of graphene oxide in aluminum powder by direct electrostatic adsorption for fabrication of graphene/aluminum composites.,” *Nanotechnology*, vol. 25, no. November, p. 325601, 2014.

[34] S. E. Shin and D. H. Bae, “Deformation behavior of aluminum alloy matrix composites reinforced with few-layer graphene,” *Compos. Part A Appl. Sci. Manuf.*, vol. 78, pp. 42–47, 2015.

[35] L. A. Yolshina, R. V. Muradymov, I. V. Korsun, G. A. Yakovlev, and S. V. Smirnov, “Novel aluminum-graphene and aluminum-graphite metallic composite materials: Synthesis and properties,” *J. Alloys Compd.*, vol. 663, pp. 449–459, 2016.

[36] J. Liu *et al.*, “Graphene oxide and graphene nanosheet reinforced aluminium matrix composites: Powder synthesis and prepared composite characteristics,” *Mater. Des.*, vol. 94, pp. 87–94, Mar. 2016.

[37] S. Timoshenko and S. Woinosky-Krieger, “Theory of Plates and Shells Classic,” p. 580, 1959.

[38] E. J. Hearn, *Mechanics of Materials 2: The mechanics of elastic and plastic deformation of solids and structural materials*. 1997.

[39] T. Laha, S. Kuchibhatla, S. Seal, W. Li, and A. Agarwal, “Interfacial phenomena in thermally sprayed multiwalled carbon nanotube reinforced aluminum nanocomposite,” *Acta Mater.*, vol.

*ORCID ID: 0000-0003-2047-5807
E-mail: Sumsun.naher.1@city.ac.uk

55, no. 3, pp. 1059–1066, 2007.

[40] L. Ci, Z. Ryu, N. Y. Jin-Phillipp, and M. Rühle, “Investigation of the interfacial reaction between multi-walled carbon nanotubes and aluminum,” *Acta Mater.*, vol. 54, no. 20, pp. 5367–5375, 2006.

[41] S. B. Prabu, L. Karunamoorthy, S. Kathiresan, and B. Mohan, “Influence of stirring speed and stirring time on distribution of particles in cast metal matrix composite,” *J. Mater. Process. Technol.*, vol. 171, no. 2, pp. 268–273, 2006.

[42] A. C. Ferrari and J. Robertson, “Interpretation of Raman spectra of disordered and amorphous carbon,” *Phys. Rev. B*, vol. 61, no. 20, pp. 14095–14107, 2000.

[43] D. Graf *et al.*, “Spatially Resolved Raman Spectroscopy of Single- and Few-Layer Graphene,” pp. 1–6, 2006.

[44] D. Graf *et al.*, “Spatially Resolved Raman Spectroscopy of Single- and Few-Layer Graphene,” pp. 1–6, 2006.

[45] T. M. G. Mohiuddin *et al.*, “Uniaxial strain in graphene by Raman spectroscopy: G peak splitting, Grüneisen parameters, and sample orientation,” *Phys. Rev. B - Condens. Matter Mater. Phys.*, vol. 79, no. 20, 2009.

[46] J. D. Renteria, S. Ramirez, H. Malekpour, B. Alonso, A. Centeno, and A. Zurutuza, “Anisotropy of Thermal Conductivity of Free-Standing Reduced Graphene Oxide Films Annealed at High Temperature,” pp. 1–28, 2015.

[47] J. Wang, Z. Li, G. Fan, H. Pan, Z. Chen, and D. Zhang, “Reinforcement with graphene nanosheets in aluminum matrix composites,” *Scr. Mater.*, vol. 66, no. 8, pp. 594–597, 2012.

[48] E. Neubauer, M. Kitzmantel, M. Hulman, and P. Angerer, “Potential and challenges of metal-matrix-composites reinforced with carbon nanofibers and carbon nanotubes,” *Compos. Sci. Technol.*, vol. 70, no. 16, pp. 2228–2236, 2010.

[49] M. a. Rafiee, J. Rafiee, Z. Wang, H. Song, Z. Z. Yu, and N. Koratkar, “Enhanced mechanical properties of nanocomposites at low graphene content,” *ACS Nano*, vol. 3, no. 12, pp. 3884–3890, 2009.

*ORCID ID: 0000-0003-2047-5807
E-mail: Sumsun.naher.1@city.ac.uk